Coded Excitation for Pulse-Echo Systems

Julio Isla and Frederic Cegla

***Abstract*— Pulse compression has been used for decades in radar, sonar, medical, and industrial ultrasound. It consists in transmitting a modulated or coded excitation, which is then cross-correlated with the received signal such that received echoes are time compressed, thereby increasing their intensity and hence the system resolution and signal-to-noise ratio (SNR). A central problem in pulse-echo systems is that while longer coded excitations yield higher SNRs, the length of the coded excitation or sequence is limited by the distance between the closest reflector and the transmitter/receiver. In this paper, a new approach to coded excitation is presented whereby receive intervals or pauses are introduced within the excitation itself; reception takes place in these intervals. As a result, the code length is no longer limited by the distance to the closest reflector and a higher SNR increase can be realized. Moreover, the excitation can be coded in such a way that continuous transmission becomes possible, which reduces the overall duration of the system response to changes in the medium. The optimal distribution of the receive intervals within the excitation is discussed, and an example of its application in industrial ultrasound is presented. The example consists of an electromagnetic–acoustic transducer driven with 4.5 V, where a clear signal can be obtained in quasi-real-time (e.g., ∼9-Hz refresh rate), while commercially available systems require 1200 V for a similar performance.**

***Index Terms*— Binary codes, electromechanical sensors, signal-to-noise ratio (SNR), ultrasonic transducers.**

I. Introduction

PULSE compression has been in use for decades to increase the signal-to-noise ratio (SNR) and resolution in radar [1], [2], sonar [3], [4], medical [5]–[11], and industrial ultrasound [12]–[17]. It consists in transmitting a modulated or coded excitation, which is then correlated with the received signal such that received echoes become shorter in duration and higher in intensity, thereby increasing the system resolution and SNR. Pulse compression is a faster alternative to averaging because a wait time is required between consecutive excitations. During this time, the energy in the medium that is being inspected dies out and therefore does not cause interference between excitations.

The two main approaches to pulse compression are chirp signals and coded excitation (or sequences). Chirp signals are obtained by frequency modulating the excitation; the increase in SNR and resolution depends on the chirp length and bandwidth [11]. Coded sequences operate in a slightly different way, most often by coding the polarity of concatenated bursts according to a binary sequence, i.e., a sequence composed of 1s and 0s or +1s and −1s [15]. In any case, a good approximation to the single initial burst is obtained when correlating the received signal with the transmitted sequence, hence the term *compression*.

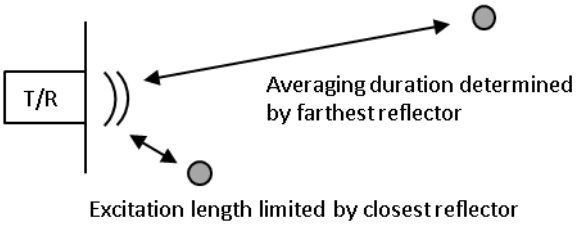

Fig. 1. Pulse-echo system with close and far reflectors.

In the applications that initially motivated this paper, namely, low-power excitation of guided ultrasonic waves [6], [16], electromagnetic–acoustic transducers (EMATs) [12], [18], photo-acoustic imaging [13], air-coupled ultrasound [14], [15], [17], [20], and piezoelectric paints [19], the received signals commonly lie below the noise threshold. Therefore, an increase in the SNR of more than 30 dB is required to accurately extract the information from the signals. The goal in those scenarios is to transmit the longest sequence or chirp signal possible to achieve the highest SNR increase, but in a pulse-echo system, the distance between the closest reflector and the transmit/receive (T/R) source limits their length. This problem is critical when reflectors are simultaneously located very close to and very far from the T/R source (see Fig. 1). In this scenario, long sequences cannot be transmitted and averaging takes a longer time due to the need for long receive intervals between transmissions so that the echoes from the farthest reflector do not overlap.

Fig. 2(a) shows a common scenario of a low-SNR pulse-echo system in industrial ultrasound affected by the problem of close and far reflectors. It consists of a metal block with a transmit–receive transducer on the front wall of the block. The objective is to find the thickness of the block, i.e., the location of the opposite parallel back wall. The back wall itself acts as the closest reflector, whereas the wave reverberation between the walls behaves as reflections from far reflectors. The received signals when using averaging are shown in Fig. 2(b). After each transmission, there are several echoes that decay progressively, and hence some wait time between transmissions is necessary to avoid interference; this makes averaging a lengthy process. Fig. 2(c) shows the received signals when transmitting a sequence or a chirp signal.

Manuscript received October 20, 2016; accepted January 24, 2017. Date of publication January 30, 2017; date of current version April 1, 2017. The work of F. Cegla was supported by EPSRC under Grant EP/K033565/1.

The authors are with the Department of Mechanical Engineering, Imperial College London, London SW72AZ, U.K. (e-mail: j.isla13@imperial.ac.uk; f.cegla@imperial.ac.uk).

Readers who are interested in accessing data associated with this paper are referred to www.imperial.ac.uk/non-destructive-evaluation where either the data or details of how to obtain the data can be found.

Digital Object Identifier 10.1109/TUFFC.2017.2661383

This work is licensed under a Creative Commons Attribution 3.0 License. For more information, see http://creativecommons.org/licenses/by/3.0/

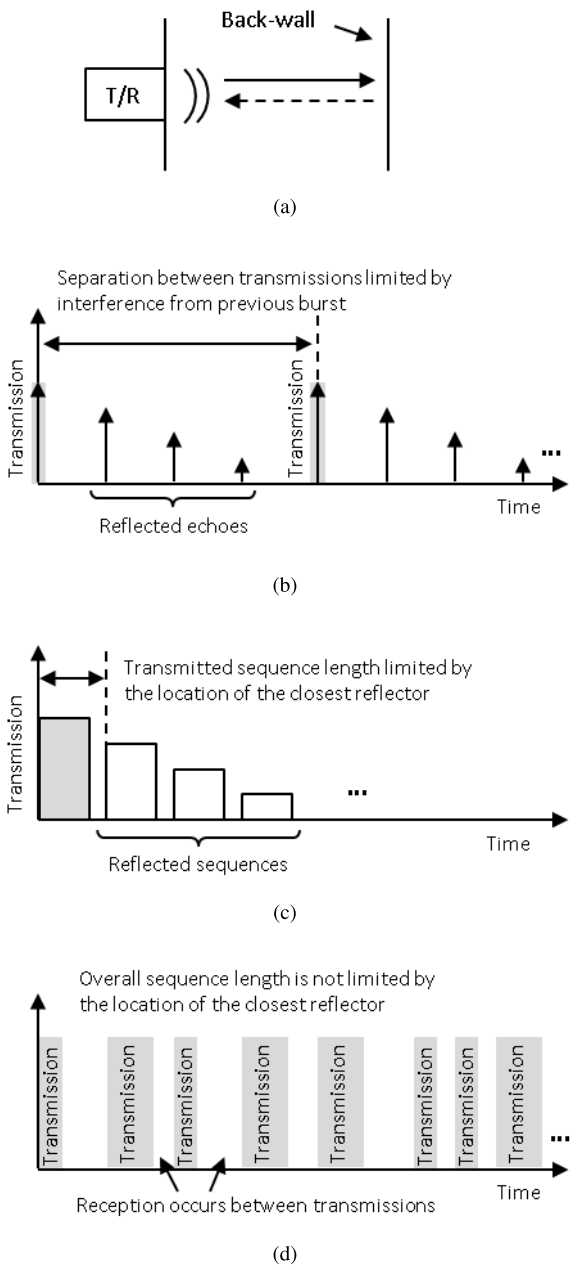

Fig. 2. Different types of excitations for pulse-echo transducers. (a) Transducer operating in pulse-echo mode. (b) Received signal when using averages. (c) Received signals when using a sequence. (d) Proposed sequence with receive intervals.

The location of the back wall limits the length of the excitation, and therefore the SNR increase. If the excitation overlaps the reflection from the back wall, the information is lost because it is not possible to receive while transmitting.

In this paper, the authors propose a solution to these problems by introducing blank gaps or intervals within a coded sequence in which reception can take place while the sequence is being transmitted [see Fig. 2(d)]. Hence, the overall sequence length and SNR increase are independent of the location of the reflectors. The aim of this idea is to increase the SNR without compromising the overall duration of the measurement so that the pulse-echo system can still respond to fast changes in the medium that is being inspected.

The organization of this paper is as follows. First, the proposed methodology is briefly introduced. Then, the autocorrelation properties of standard sequences and the corresponding SNR increase are discussed in Section III. The properties and construction of coded sequences that have receive intervals are introduced in Section IV. In Section V, the experimental results are presented. After discussing the results, conclusions are drawn in Section VI.

II. Overview of Proposed Coded Excitation

Fig. 3 shows the fundamental steps of the proposed methodology. There are three main stages: 1) sequence synthesis; 2) propagation through the medium and reception; and 3) postprocessing. First, two sequences are generated, sequence $\mathbf{X}$ controls the polarity of the burst ($+1$ or -1), whereas $\mathbf{G}$ controls the T/R intervals (1 corresponds to transmission and 0 to reception).

In practice, the transmitted sequences are not a train of delta functions but concatenated band-limited bursts, $\mathbf{B}$. These band-limited bursts are necessary due to the limited bandwidth of the electronics and transducers. The bursts are assumed to be optimal; this means that their length can be the maximum possible without overlapping the closest reflector and that it can utilize all the available bandwidth. Moreover, there is no restriction on the type of burst; they can be square pulses, chirp signals, or multiple cycles with a certain apodization.

Before the sequences can be modulated by the burst $\mathbf{B}$, they have to be upsampled by Q samples to match the burst length. By doing so, $\mathbf{X}'$ and $\mathbf{G}'$ are obtained. Then $\mathbf{X}'$ is convolved with $\mathbf{B}$, which yields $\mathbf{X}''$. On the other hand, $\mathbf{G}'$ is convolved with a rectangular pulse, which gives $\mathbf{G}''$. The transmitted sequence $\mathbf{Z}''$ is simply the multiplication of the elements of $\mathbf{X}''$ and $\mathbf{G}''$.

The reflected signals can be modeled as the convolution of the medium impulse response and the excited sequence $\mathbf{Z}''$; an example is shown in Fig. 3. At the receiver, the reflected signals are combined with noise from the electronics $\mathbf{Y}$. The complement $\overline{\mathbf{G}}'' = 1 - \mathbf{G}''$ is used to zero the received signal when transmission is on. This is basically the role of the T/R switch in the electronics. In practice, the T/R switching occurs before the receiver noise is added to the signal; however, in Fig. 3, the order of the operation is flipped to indicate that reception does not take place during transmission and the signals are zeroed. Recall that transmission and reception cannot occur simultaneously in pulse echo due to the limited dynamic range of the receiver.

The modulated medium response can be partially recovered by cross correlating the received signals with $\mathbf{X}' \cdot \mathbf{G}'$; this is the compression stage. Note that cross correlation is equivalent to convolution with one of the terms being time reversed. The recovered medium response will have a noise component (not shown in Fig. 3) that corresponds to the electronics. Interference between bursts in the sequence will also affect the recovered medium response. Further noise reduction is possible by cross correlating the result with the burst $\mathbf{B}$, which is the matched-filtering stage. However, matched filtering distorts the originally transmitted burst, as can be appreciated in Fig. 3.

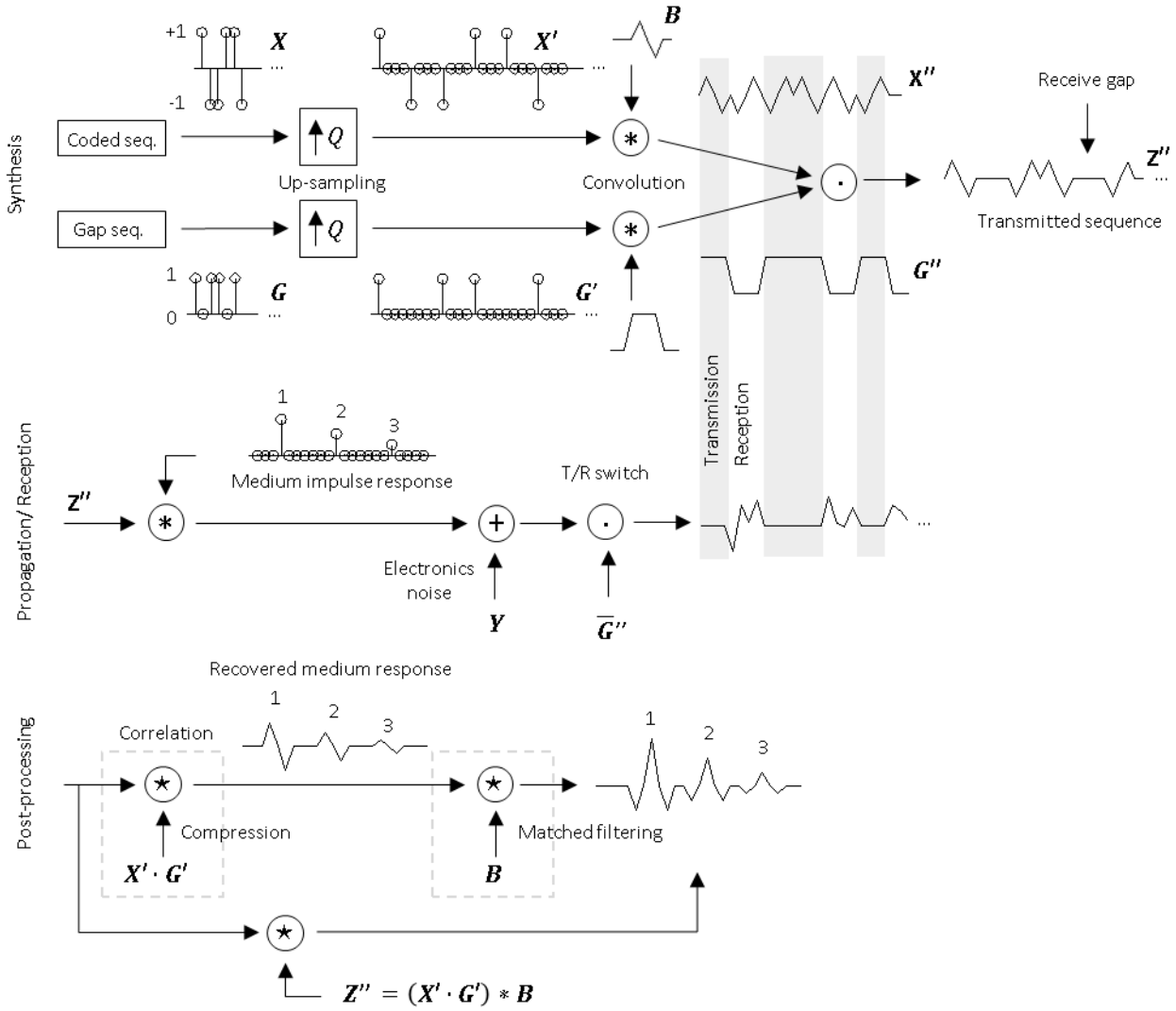

Fig. 3. Fundamental steps of the proposed coded excitation. The operators {·}, {∗}, and {⋆} indicate multiplication, convolution, and cross correlation, respectively.

It has to be highlighted that the steps in Fig. 3 have been arranged in such a way that they correspond to fundamental steps of the methodology proposed so that it is easier to understand; however, this is not necessarily an efficient way of implementing it. For example, $\mathbf{Z}''$ can be obtained by simply convolving $\mathbf{B}$ with the upsampled result of $\mathbf{X} \cdot \mathbf{G}$ and the last compression and matched-filtering operations combined, which is equivalent to cross correlating the received signal with the transmitted signal $\mathbf{Z}'' = (\mathbf{X}' \cdot \mathbf{G}') * \mathbf{B}$, where {∗} indicates convolution.

In the next sections, we investigate the optimal synthesis of these random sequences that have receive intervals and their expected SNR.

III. Background on Coded Excitation

In this section, we focus our attention on coded sequences, especially binary coded sequences, whereby the polarity of the sequence burst (or symbol) is changed. These are simpler to implement than nonbinary ones. There are no restrictions on the bursts other than their bandwidth not exceeding that of the system and their length not overlapping the closest reflector; note a burst can be a chirp signal. In this section, we review the previous work on coded sequences and then discuss their *merit factor*; this is central to proving the optimality of the sequences with receive intervals proposed in this paper.

A. Previous Work

Overall, the performance of a sequence relies on its autocorrelation properties. Ideally, its autocorrelation should be a delta function, but this cannot be achieved with a single sequence. The quest for "good" sequences started around the middle of the last century [21]–[24] and still continues today [25]–[27] (see [28]–[30] for a comprehensive review of the different sequences). Among the key binary sequences known so far are those named after Barker [31], those reported by Leung and Schmidt [32] and Hoholdt and Jense [33], as well as maximum length register sequences [34]. This list is not exhaustive and other sequences can be found in the literature [29], though some may be considered either as special cases or family members of those previously mentioned.

One of the most elegant solutions to the imperfection of the autocorrelation properties of a single sequence can be found in [21], whereby paired complementary sequences produce a perfect delta function when their corresponding autocorrelations are added together; this was later extended to orthogonal complementary sets of sequences in [22]. Another solution is to use sequences that achieve zero or very low autocorrelation values only in certain intervals of interest [35]–[39]. In general, there has been a tremendous interest in improving the autocorrelation properties of sequences, mainly by means of optimization strategies (see [26], [38]–[43]), and also in efficient ways of processing and obtaining them [37], [44], [45].

The fact that good or perfect autocorrelation can be partially achieved is highly relevant; however, there are certain scenarios where the SNR at the input of the amplifier is low [6], [12]–[16], [18]–[20], [46], and in these cases, good autocorrelation properties are not essential. Indeed, in this section, it is shown that when the SNR is low (i.e., the signal magnitude is comparable to or below the noise level), the choice of the sequence is relatively unimportant and a simple random sequence that has a uniform distribution of $+1$s and -1s will suffice in most cases.

B. Merit Factor

Let $\mathbf{X}$ be a sequence of N elements, where each element x takes on values $+1$ or -1. The aperiodic autocorrelation of this sequence at shift k is

$$c_k = \sum_{j=0}^{N-k-1} x_j x_{j+k}, \quad k = 0, \cdots, N-1. \tag{1}$$

Golay [47] introduced the *merit factor, F,* of a sequence to compare and measure its performance

$$F = \frac{N^2}{2\sum_{k=1}^{N-1} c_k^2}. \tag{2}$$

The merit factor is basically the ratio between the energy at shift zero and the combined energy of the rest of the shifts or autocorrelation sidelobes. The factor 2 is included to compensate for the tapering effect of the aperiodic autocorrelation. The merit factor can be understood as a measure of how similar the autocorrelation result is to a delta function; for the sake of simplicity, it should be assumed that the elements c_k, $k \in [1, N-1]$, have a zero mean. A random binary sequence with $+1$s and -1s has $F \approx 1$ on average for large N [47]; a Barker sequence of 13 elements, which is the longest known, has $F \approx 14.08$ [32], [33]; Golay sequences [47] have $F \approx 3$, the added autocorrelations of the Golay complementary sequences have of course $F = \infty$, while Legendre sequences can achieve $F \approx 6$ [33].

Finding sequences with an optimal merit factor for a given length by extensive search is computationally demanding; the best known cases from 60 to 200 elements are limited to $F \approx 10$ [29], [30]. Longer sequences are expected to have $\max\{F\} < 6$ since no sequence with a higher merit factor has been found, though this remains a conjecture [30].

C. SNR Increase

When adding (averaging) N received signals from identical excitations, the resulting SNR is

$$\mathrm{SNR}_{\mathrm{avg}} = N \cdot \mathrm{SNR}_{\mathrm{in}} \tag{3}$$

where the input SNR, $\mathrm{SNR}_{\mathrm{in}}$, is defined as

$$\mathrm{SNR}_{\mathrm{in}} = \frac{s^2}{\sigma_{\mathrm{in}}^2} \tag{4}$$

where s is the magnitude of the received signal, assuming that the excitation is an impulse and that there is only one point-like reflector, and σ_{in}^2 is the variance of the received noise, which has zero mean. In most ultrasound systems, the received noise is mainly due to noise of the receive amplifier—for simplicity, this noise can be assumed to be additive white Gaussian noise. Clearly, the actual received signal can take on other values after noise is added, but here s refers to the ideal received signal prior to additive noise.

In order to simplify the analysis and to focus the attention on the sequences themselves, two assumptions have been made: 1) the excitation is an impulse and 2) there is only one point-like reflector. This means that the receive sequence only takes on $+s$ and $-s$ values. We discuss the effect of modulation and multiple reflectors in Section IV-F.

When using coded excitation, the cross correlation of the received signal and the transmitted sequence introduces noise as a result of the interference between the coded bursts in the sequence. This interference is of (pseudo) random nature and behaves similarly to the electrical noise of the receiver. Therefore, it is referred to simply as noise and measured in the same way since its effect is not different from that of electrical noise.

Let the transmitted sequence be of length N with unity magnitude and let the received sequence take on values $+s$ and $-s$. Then, the energy at shift $k = 0$ after cross correlation is $(N \cdot s)^2$, while the sample variance of the noise introduced by the cross correlation is σ_s^2, which can be defined as

$$\sigma_s^2 = \frac{2s^2}{N-1} \sum_{k=1}^{N-1} c_k^2 \approx \frac{N \cdot s^2}{F} \tag{5}$$

when N is large. The factor 2 in (5) has been added to compensate for the tapering effect the aperiodic cross correlation has on c_k.

Now, let $\mathbf{Y}$ be a sequence of independent and identically normally distributed (i.i.d.) elements y_j with zero mean and variance σ^2; say this sequence represents the noise added at the receiver. The sample variance of the result of cross-correlating $\mathbf{Y}$ with the transmitted sequence can be approximated, if N is large, to

$$\sigma_{\mathrm{Y}}^2 \approx \mathrm{E}\left[\frac{2}{N-1} \sum_{k=1}^{N-1} d_k^2\right] \tag{6}$$

where $E[\cdot]$ denotes the expected value and d_k are the coefficients of the cross correlation for each shift k. Since each d_k is

i.i.d. with zero mean

$$\sigma_{\mathrm{Y}}^2 \approx \frac{2}{N-1}\sum_{k=1}^{N-1} E\left[d_k^2\right] \tag{7}$$

$$d_k = \sum_{j=0}^{N-k-1} y_j x_{j+k}, \quad k \in [1, N-1]. \tag{8}$$

Due to each y_j and x_{j+k} being also i.i.d. with zero mean, we have

$$E\left[d_k^2\right] = \sum_{j=0}^{N-k-1} E\left[y_j^2\right] E\left[x_{j+k}^2\right] = \sigma^2(N-k), \quad k \in [1, N-1]. \tag{9}$$

Hence

$$\sigma_Y^2 \approx N\sigma^2. \tag{10}$$

Finally, given that the noise introduced by the sequence is independent of the noise introduced by $\mathbf{Y}$, the SNR of the aperiodic cross correlation can be approximated, when N is large, as

$$\mathrm{SNR_s} = \frac{(N\cdot s)^2}{\sigma_s^2 + \sigma_Y^2} \approx \frac{N}{\frac{1}{F} + \frac{1}{\mathrm{SNR_{in}}}}. \tag{11}$$

There are two special cases of interest in (11)

$$\mathrm{SNR_s} \approx \begin{cases} N\cdot \mathrm{SNR_{in}}, & \text{if } F \gg \mathrm{SNR_{in}} \\ N\cdot F, & \text{if } F \ll \mathrm{SNR_{in}}. \end{cases} \tag{12}$$

If $F \gg \mathrm{SNR_{in}}$, the SNR increase due to coded excitation is that of averaging [see (3)]. Moreover, *there is no benefit in using sequences with* $F > 1$ *(i.e., other than random sequences, which achieve* $F \approx 1$ *when* N *is large) to increase the SNR when* $\mathrm{SNR_{in}} \ll 1$. Note that even the complementary Golay sequences, which can perfectly cancel the sequence noise [21], [22], yield no advantage in this case.

Interestingly, many scenarios exist where either $\mathrm{SNR_{in}} \sim 1$ or $\mathrm{SNR_{in}} \ll 1$ and hence a significant number of averages or long sequences are required (commonly $N > 1000$) to produce a satisfactory SNR, which often need to be on the order of 30–50 dB. These scenarios are usually found in systems that rely on inefficient/poor transducers or have constraints on the excitation power [6], [12]–[16], [18]–[20], [46].

Conversely, if $F \ll \mathrm{SNR_{in}}$, the $\mathrm{SNR_s}$ is independent of $\mathrm{SNR_{in}}$, and if $\mathrm{SNR_{in}}$ is high, it may happen that $\mathrm{SNR_{in}} > \mathrm{SNR_s}$ for a given N due to the noise introduced by the sequence during the cross-correlation operation. In these cases, special attention should be paid to increasing the merit factor F and hence to the use of complementary Golay sequences and zero autocorrelation zone sequences [35]–[39].

IV. Properties and Synthesis of Sequences With Receive Intervals

In a pulse-echo system, the length of the excitation, be that a coded sequence or a chirp signal, is limited by the distance between the closest reflector and the T/R source (see Fig. 1). In order to transmit longer sequences, intervals where reception can take place can be introduced in the sequences.

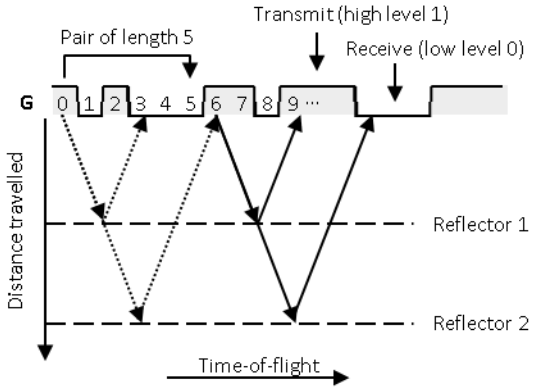

Fig. 4. Random distribution of receive intervals in a sequence. A burst is sent in each transmit interval (sequence **G** high level) and the reflected echo can be received only if its arrival time matches the occurrence of a receive interval (sequence **G** low level).

In this section, the rationale behind this approach is explained and the optimal distribution of the receive intervals within a given sequence is discussed.

A. Synthesis of Sequences With Receive Intervals

It is desirable to create a ternary random sequence $\mathbf{Z}$ that takes on values $+1$, -1, and 0, where the values $+1$ and -1 codify the excitation and the zeroes permit reception to take place, hence the name receive interval. Such a ternary sequence can be synthesized as follows. Let $\mathbf{X}$ be a binary sequence of length L that takes on values $+1$ and -1 and let $\mathbf{G}$ be another binary sequence also of length L that takes on values $+1$ and 0. Sequence $\mathbf{Z}$ can be obtained as

$$\mathbf{Z} = \mathbf{X}\cdot\mathbf{G} = (x_0 g_0, x_1 g_1, \ldots, x_{L-1} g_{L-1}) \tag{13}$$

where each x_j and g_j are i.i.d.. The process described by (13) is shown in Fig. 3 including the burst modulation. The sequence $\mathbf{G}$ controls the location of the receive intervals ($g_j = 0$) and transmit intervals ($g_j = 1$), whereas $\mathbf{X}$ controls the polarity (± 1) of the bursts during the transmit interval. For simplicity, and without loss of generality, each T/R interval is considered to be of the same length. The expected SNR when using $\mathbf{Z}$ is quantified in Section IV-C, where each term of (13) is instrumental in the mathematical formulation.

Now we introduce the concept of transmit–receive pairs within the sequence $\mathbf{G}$. The transmit–receive pairs are responsible for the amount of energy received from reflectors, which is discussed in Section IV-B. Let $\overline{g}_j$ be the complement of g_j defined as

$$\overline{g}_j = 1 - g_j \tag{14}$$

then $\{g_j, g_{j+m}\}$ *is said to be a transmit–receive pair of length* m if $g_j \overline{g}_{j+m} = 1$. As an example, a pair of length $m = 5$ is shown in Fig. 4.

The pair length is defined as a range of time differences between any two transmit and receive states. Therefore, a given pair length corresponds to the total travel time range of a wave to and back from a potential reflector. The larger the pair length, the longer the travel time, and hence the deeper the potential reflector. The amount of energy received from a

given reflector is proportional to the total number of transmit and receive pairs of a pair length that corresponds to the depth of the reflector. For this reason, a uniform probability distribution of pair lengths is desired in order to have a uniform sensitivity with respect to the reflector depth. In the next section, it is discussed how to ensure this condition, whereas the expected amount of energy received from a given reflector is investigated in Section IV-C.

Fig. 4 shows an example of a sequence $\mathbf{G}$ together with the time-of-flight and distance traveled by waves generated in transmit intervals of $\mathbf{G}$. For example, the wave generated in g_0 reflects back from reflectors 1 and 2 and the first reflection arrives at g_3, so this reflector location is said to require a pair of length $m = 3$. Similarly, the second reflection arrives at g_6, and hence this reflector is said to require a pair $m = 6$.

In a pulse-echo system, where transmission and reception cannot occur simultaneously due to the limited dynamic range of the receiver, a transmit–receive pair may not exist for a given transmit interval and reflector location. For example, in Fig. 4, $\{g_0, g_6\}$ is not a valid pair because $g_0\overline{g}_6 = 0$ and hence the reflection cannot be received.

B. Random Distribution of Receive and Transmit Intervals for Even Sampling of the Medium

In a pulse echo system, it is important to ensure equal sensitivity to every reflector regardless of its location in the interrogated space. When using the sequences with receive intervals and ignoring beam spread and directivity effects, this is equivalent to obtaining the same number of reflections, i.e., the same amount of energy, from any point-like reflector irrespective of its location. More formally, this is to obtain the same number of reflections r for any transmit–receive pair of length m up to a length M.

This condition can approximately be satisfied by any random binary sequence $\mathbf{G}$ when L is large and $L \gg M$. To prove this, let the expected number of reflections that correspond to a reflector, whose distance from the transducer corresponds to a transmit–receive pair of length m, be

$$r_m = E\left[\sum_{j=0}^{L-m-1} g_j \overline{g}_{j+m}\right] \quad m \in [1, M]. \tag{15}$$

Note that r_m is basically the expected total number of valid transmit–receive pairs, i.e., those that yield $g_j\overline{g}_{j+m} = 1$, for each shift m.

Let p_1 be the probability of having a transmit interval defined as

$$p_1 = E[g_j] = 1 - E[\overline{g}_j]. \tag{16}$$

As every g_j in (15) is i.i.d.

$$r_m = p_1(1 - p_1)(L - m) \quad m \in [1, M]. \tag{17}$$

Then if $L \gg M$

$$r = r_m|_{L \gg M} \approx p_1(1 - p_1)L. \tag{18}$$

In practice, the location of the furthest reflector is limited to an equivalent transmit–receive pair of length M. By using sequences of length $L \gg M$, the number of reflections from any possible reflector location within such a finite distance can be homogenized, as shown by (18). This greatly simplifies the formulas for the quantification of the sequence SNR in the next section.

C. SNR and Optimal Ratio of Transmit and Receive Intervals

Having discussed that a random distribution of transmit–receive intervals guarantees that the same number of reflections r be received irrespective of the reflector location within a finite distance from the source, the next step is to investigate the optimal number or proportion of transmit–receive intervals in a sequence, i.e., find the optimal p_1. The optimal number of transmit intervals p_1L is that which yields the maximum SNR for a given sequence $\mathbf{G}$ of length L. To obtain the SNR of a sequence with receive intervals, the total received energy, the noise from the sequence and the added noise at the receiver need to be found as follows.

Let $\mathbf{Y}$ be the noise added at the receiver. To estimate the sample variance after the cross correlation of $\mathbf{Y}$ with the transmitted sequence $\mathbf{Z}$, σ^2_{YG}, the steps from (6) to (10) can be repeated. When M is large, σ^2_{YG} can be approximated as

$$\sigma^2_{YG} \approx \frac{1}{M}\sum_{k=1}^{M} e_k^2 \approx E[e_k^2] \quad M \ll L, \tag{19}$$

where e_k are the coefficients of the cross correlation for each shift k. Note that the factor 2 has been dropped with respect to (6) because $M \ll L$ shifts are used to obtain σ^2_{YG}, and therefore, the tapering effect of the cross correlation can be neglected.

$$E[e_k^2] = \sum_{j=0}^{L-k-1} E\left[z_j^2 \overline{g}_{j+k} y_{j+k}^2\right]. \quad k \in [1, M], \tag{20}$$

where $z_j = x_j g_j$ are the elements of $\mathbf{Z}$ and $\overline{g}_j y_j$ are the elements of the received sequence; note that $\overline{g}_j^2 = \overline{g}_j$. Finally,

$$\sigma^2_{\mathrm{YG}} \approx r\sigma^2 \quad M \ll L. \tag{21}$$

Now the sample variance of the noise introduced by the sequence itself is investigated following the same steps. Say M is large, then

$$\sigma^2_{SG} \approx \frac{1}{M}\sum_{k=1}^{M} f_k^2 \approx E\left[f_k^2\right] \quad M \ll L, \tag{22}$$

where f_k are the coefficients of the cross correlation for each shift k and

$$E\left[f_k^2\right] = s^2 \sum_{j=m}^{L-k-1} E\left[z_j^2 \overline{g}_{j+k} z_{j-m+k}^2\right], \quad m \in [1, M] \tag{23}$$

where $z_{j-m}s = g_{j-m}x_{j-m}s$ are the elements of the reflected sequence (i.e., the transmitted sequence z_j scaled by s and shifted by m) while the actual received sequence is $\overline{g}_j z_{j-m}s$. Note that

$$\sigma^2_{SG} \approx p_1 r s^2 \quad M \ll L. \tag{24}$$

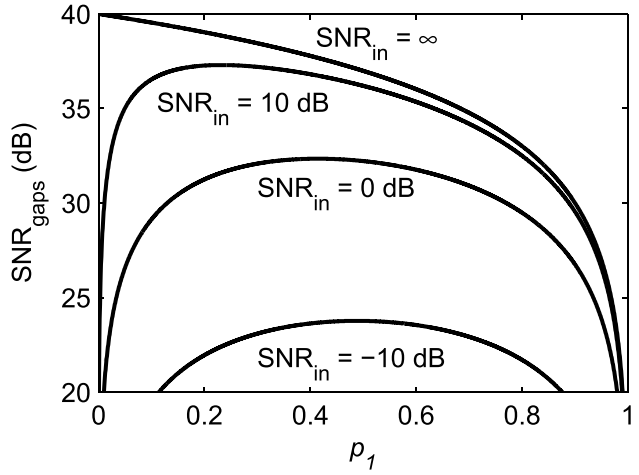

Fig. 5. SNR of the sequence with receive intervals, $\mathrm{SNR}_{\mathrm{gaps}}$, versus the probability of having a transmit interval p_1 for different input SNRs, $\mathrm{SNR}_{\mathrm{in}}$. The total length of the sequence is set to $L = 10^4$.

According to (18), r reflections are received, and since each reflection has magnitude s, the total received energy at shift $k = m$ is approximately $(r \cdot s)^2$ when $L \gg M$. Hence, when M is large and $L \gg M$

$$\mathrm{SNR}_{\mathrm{gaps}} \approx \frac{(r \cdot s)^2}{\sigma_{SG}^2 + \sigma_{YG}^2} \approx \frac{r}{p_1 + \frac{1}{\mathrm{SNR}_{\mathrm{in}}}}. \tag{25}$$

Fig. 5 shows $\mathrm{SNR}_{\mathrm{gaps}}$ versus p_1 for different $\mathrm{SNR}_{\mathrm{in}}$; L has been set to 10^4 to provide a numerical example. There are two extreme cases of interest

$$\mathrm{SNR}_{\mathrm{gaps}} \approx \begin{cases} r \cdot \mathrm{SNR}_{\mathrm{in}}, & \text{if } \mathrm{SNR}_{\mathrm{in}} \ll \frac{1}{p_1} \\ (1 - p_1)L, & \text{if } \mathrm{SNR}_{\mathrm{in}} \gg \frac{1}{p_1}. \end{cases} \tag{26}$$

Given that $\max\{r\} = 0.25L$, which occurs for $p_1 = 0.5$, then $\max\{\mathrm{SNR}_{\mathrm{gaps}}\}|_{\mathrm{SNR}_{\mathrm{in}} \ll 2} = 0.25L \cdot \mathrm{SNR}_{\mathrm{in}}$. Conversely, if $\mathrm{SNR}_{\mathrm{in}} \gg 1/p_1$, $\mathrm{SNR}_{\mathrm{gaps}}$ is independent of $\mathrm{SNR}_{\mathrm{in}}$, and if $\mathrm{SNR}_{\mathrm{in}}$ is high, it may happen that $\mathrm{SNR}_{\mathrm{in}} > \mathrm{SNR}_{\mathrm{gaps}}$, in which case the use of the sequences is detrimental.

Moreover, $\mathrm{SNR}_{\mathrm{gaps}}$ is a concave function of p_1 for any $\mathrm{SNR}_{\mathrm{in}} < \infty$. Then, there exists a value of p_1 that maximizes $\mathrm{SNR}_{\mathrm{gaps}}$ for each $\mathrm{SNR}_{\mathrm{in}}$

$$p_{1,\max} = \arg\max_{p_1} \{\mathrm{SNR}_{\mathrm{gaps}}\} \leq 0.5 \tag{27}$$

and hence the maximum $\mathrm{SNR}_{\mathrm{gaps}}$ is

$$\mathrm{SNR}_{\mathrm{gaps,max}} \approx \frac{(1 - p_{1,\max})L}{1 + \frac{1}{p_{1,\max}\mathrm{SNR}_{\mathrm{in}}}}. \tag{28}$$

An important fact is that $p_1 = 0.5$ performs nearly optimally once $\mathrm{SNR}_{\mathrm{in}} < 0$ dB.

The figure of merit of the sequence F was not included in (25) because this equation is intended to be used with random sequences that do not have any predefined structure and for which $F \approx 1$ when L is large. This is because we conjecture that it should be difficult to obtain a sequence that produces $F > 1$ when random receive intervals are used due to the structure of the transmitted sequence being affected by these intervals.

Finally, it is worth mentioning that sequences whose elements take on values $+1$, -1 and 0 have been reported in the literature and are known as ternary sequences [48]–[50]. However, the insertion of the zeroes aims to improve the sequence autocorrelation properties and is not initially intended for reception to take place. Furthermore, these sequences do not necessarily satisfy $p_1 = 0.5$, which is required for optimal performance when $\mathrm{SNR}_{\mathrm{in}} \ll 2$.

D. Comparison Between Sequences With Receive Intervals and Averaging

Once we assume that the sequence burst is optimal (i.e., its length can be the maximum possible without overlapping the closest reflector and it can utilize all the available bandwidth) and that the sequence burst can also be a chirp signal, averaging using the same sequence burst is the only relevant comparison point against the sequences with receive intervals. In this section, we investigate which of these techniques yields the highest SNR increase in a given amount of time subject to $\mathrm{SNR}_{\mathrm{in}}$. To do so, we introduce the following ratio:

$$\alpha = \frac{\mathrm{SNR}_{\mathrm{gaps,max}}}{\mathrm{SNR}_{\mathrm{avg}}} \approx \frac{1 - p_{1,\max}}{t\left(\mathrm{SNR}_{\mathrm{in}} + \frac{1}{p_{1,\max}}\right)}, \tag{29}$$

$$t = \frac{N}{L}, \tag{30}$$

where L is the total number of transmit and receive intervals for both the sequences and averaging, which corresponds to the total duration of the measurement. For the case of averaging, N is the number of averages that take place during the L intervals; the number of receive intervals $(L - N)$ is dictated by the need of a wait time to allow the waves in the medium to die out and hence avoid interference between averages. For example, if $t = 1/4$, then the wait time between averages necessary to avoid interference is 4 intervals or less (1 transmit and 3 receive intervals). Note that the number of transmit intervals in a sequence of length L is $p_1 L$, or $p_{1,\max} L$ in the case of (29). As before, transmit and receive intervals are considered of equal length without loss of generality.

Fig. 6 shows the values of t and $\mathrm{SNR}_{\mathrm{in}}$ for which $\alpha \approx 1$. For any combination of t and $\mathrm{SNR}_{\mathrm{in}}$ values below the curve, $\alpha > 1$, and hence the sequences with receive intervals produce a greater SNR; otherwise, averaging produces a higher SNR. A desired t for a given $\mathrm{SNR}_{\mathrm{in}}$ may not be achieved when averaging due to many receive intervals being required to avoid interference between transmissions, e.g., when wave reverberations inside the specimen are significant.

Consider the extreme case in (29), where $\mathrm{SNR}_{\mathrm{in}} \ll 2$ and for which $p_1 = 0.5$ is known to be optimal, then

$$\alpha|_{\mathrm{SNR}_{\mathrm{in}} \ll 2,\, p_1 = 0.5} \approx \frac{1}{4t}. \tag{31}$$

This means that when $t < 1/4$, i.e., when the wait time between averages necessary to avoid interference is greater than four intervals (one transmit and three receive intervals), the sequence with receive intervals produces a greater SNR. Finding scenarios where there is no interference using three

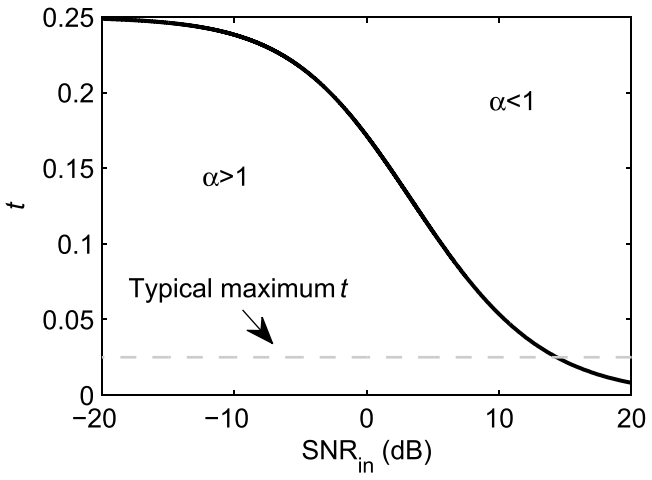

Fig. 6. Ratio of transmit and total number of intervals when averaging, $t = N/L$, and input SNR, $\mathrm{SNR_{in}}$, for which the SNR obtained after using the sequences with receive intervals is approximately the same as that of averaging, i.e., $\alpha \approx 1$. For any combination of t and $\mathrm{SNR_{in}}$ values below the curve, $\alpha > 1$, and hence the sequences with receive intervals produce a greater SNR than averaging. The dashed gray line corresponds a typical maximum t showing that for inputs with $\mathrm{SNR_{in}} < 10$ dB, the sequences with receive intervals outperform averaging.

or less receive intervals when averaging is rare in practice. A common scenario in pulse-echo ultrasound systems is to use more than 40 receive intervals when averaging—the receiver is ON for 40 times the transmit length to avoid interference. In such a case, the SNR achieved by the sequence can be at least 20 dB greater provided $\mathrm{SNR_{in}} \ll 2$ and $p_1 = 0.5$.

E. Periodic Sequences With Receive Intervals: Continuous Transmission

Let the sequence $\widehat{\mathbf{Z}}$ be infinite with period L and elements

$$\widehat{z}_{j+qL} = z_j, \quad j \in [0, L-1], \tag{32}$$

where q is an integer and the elements z_j are defined in (13). In the same way, $\widehat{g}_j$ can be defined from g_j.

Say $\widehat{\mathbf{Z}}$ is transmitted and the received signal is cross correlated with $\widehat{\mathbf{Z}}$ shifted by n. The expected value of the periodic cross correlation of a finite number of samples L is then

$$\begin{aligned} E[\widehat{f}_{k,n}] &= s \sum_{j=0}^{L-1} E\left[\widehat{z}_{j-n}\overline{\widehat{g}}_{j-n+k}\widehat{z}_{j-m+k}\right] \\ &= \begin{cases} r \cdot s, & k = m - n + qL \\ 0, & \text{otherwise,} \end{cases} \quad m, k \in [1, L-1]. \end{aligned} \tag{33}$$

Since $\widehat{\mathbf{Z}}$ and $\widehat{\mathbf{G}}$ have period L, for every n, there exists a value of k in the interval $[1, L-1]$ for which $E[\widehat{f}_{k,n}] = r \cdot s$. This means that the sequence $\widehat{\mathbf{Z}}$ can be transmitted continuously, and at any instant n, reflections within a time-of-flight of $m < L - 1$ can be recovered after cross correlating L received elements. Note the same $\mathrm{SNR_{gaps}}$ is obtained when replacing $\mathbf{Z}$ by $\widehat{\mathbf{Z}}$.

By transmitting a sequence with finite period L, a significant amount of memory and computing power is saved but the time-of-flight of the furthest reflection has to be less than $L-1$ to prevent these reflections from being seen as coherent interference. This is equivalent to waiting for the energy in a specimen to die out between transmissions when using averaging. The importance of being able to transmit/receive continuously is that it significantly reduces any delays in the system when processing the sequences, which subsequently reduces the time the system takes to respond to changes in the medium.

F. Burst Modulation and Multiple Reflectors

Let s_i be the magnitude of the received echo from reflector i, then (25) can be rewritten for a reflector i' as

$$\mathrm{SNR}'_{\mathrm{gaps}} \approx \frac{L(1-p_1)}{\sum_{i=1}^{R} s_i^2 + \frac{1}{p_1 \mathrm{SNR_{in}}}} \tag{34}$$

where R is the total number of reflectors, the reflectors are assumed to be well resolved, and $\mathrm{SNR_{in}}$ is defined with respect to $s_{i'}$. The existence of multiple reflectors increases the sequence noise; however, this increase is not significant if there are just a few dominant reflectors, as happens to be the case in most practical scenarios.

To include the effect of the burst modulation, let us assume that the sequences are upsampled to match the burst length, as shown in Fig. 3; that the normalized modulated burst $\mathbf{B}$ has variance σ_B^2 and mean zero; and that the received sequences are correlated with the upsampled but unmodulated sequences $\mathbf{X}' \cdot \mathbf{G}'$ in the compression stage, as shown in Fig. 3. This process can be understood as a shifted combination of the transmitted sequence weighted by the burst samples. Since only the peak of the burst is of interest in the numerator, this process has no effect on it. Note that only the transmitted sequences are modulated, which has no effect on the right-hand term of the denominator either. Hence, the result of the modulation on transmission is simply the variance σ_B^2 multiplying the left-hand term of the denominator

$$\mathrm{SNR}''_{\mathrm{gaps}} \approx \frac{L(1-p_1)}{\sigma_B^2 \sum_{i=1}^{R} s_i^2 + \frac{1}{p_1 \mathrm{SNR_{in}}}}. \tag{35}$$

Typically, $\sigma_B^2 \sim 0.2$ for normalized bursts, so modulation reduces the sequence noise at the expense of longer excitations.

It should be highlighted that discontinuities may occur between adjacent intervals. The magnitude of the discontinuities is given by the following.

1) The difference in the number of reflections of two contiguous transmit–receive pair lengths—for very long sequences, this difference is negligible and can also be compensated on the postprocessing stage because the number of reflections from every transmit–receive pair length is known *a priori*.
2) The phase change of the electronics noise between nonadjacent receive intervals due to the noise being band limited.

Overall, the effect of these discontinuities is negligible and can be further attenuated by filtering.

An additional SNR increase is possible using matched filtering (see Fig. 3). The effect of matched filtering on

the SNR can be found elsewhere (see [51]). Basically, if the signal is assumed to have a white noise component, mainly due to the electronics noise, the increase in the SNR corresponds to the energy of the burst. However, this result cannot be immediately extrapolated to the noise introduced by the sequences because it mostly shares the same frequency band of the burst. We found empirically that an acceptable approximation of the resulting sequence noise (left-hand term of the denominator) is as follows:

$$\mathrm{SNR}'''_{\mathrm{gaps}} \approx \frac{L(1-p_1)Q\sigma_B^2}{2Q\sigma_B^2\sigma_{BB}^2\sum_{i=1}^{R}s_i^2+\frac{1}{p_1\mathrm{SNR}_{\mathrm{in}}}}, \tag{36}$$

where Q is the number of samples of the burst and σ_{BB}^2 is the variance of the normalized autocorrelation of the burst. It is interesting to note that when the left-hand term of the denominator is negligible, which corresponds to a regime where the sequences perform optimally, the SNR increase due to matched filtering is $Q\sigma_B^2$, i.e., the energy of the burst.

V. Application Example: Fast Low-Power EMAT

In this section, a sequence with receive intervals was applied to an industrial ultrasound example, which consists of an EMAT driven with only 4.5 Vpp (peak-to-peak) and less than 0.5 W. The main advantage of using EMATs is that unlike standard piezoelectric transducers, they do not require direct contact with the specimen. However, EMATs are notorious for requiring very high excitation voltages, commonly in excess of a few hundred volts and powers greater than 1 kW [52]–[56]. In certain scenarios, high powers are not permissible, e.g., in explosive environments, such as refineries, or where compact/miniaturized electronics is wanted. Moreover, high-power electronics requires bigger components and more space to dissipate the heat. The use of sequences with receive intervals presented in this paper can be used to reduce the excitation power while keeping the overall duration of the measurement short in these scenarios.

A. Experimental Setup

The experiment setup is shown in Fig. 7(a) and (b). An EMAT (Part No. 274A0272, Innerspec, USA) was placed on top of a mild steel block, which has a thickness of 20 mm. This is a pancake coil EMAT that generates radially polarized shear waves within a circular aperture, which has an outer diameter of roughly 20 mm.

The main objective of this setup is to obtain a signal that can be used to estimate the thickness of the steel block. In this particular case, it is convenient to use the coded sequences with receive intervals because of the following reasons.

1) The back wall can be close and therefore long chirp signals or standard sequences cannot be used.
2) The steel block offers low attenuation to the wave, which reverberates inside the specimen for a long time, making averaging lengthy due to the wait time needed between transmissions.

A custom-made transmit–receive electronic circuit was developed for the experiment. This circuit was solely powered by the USB port of a standard personal computer (PC), which

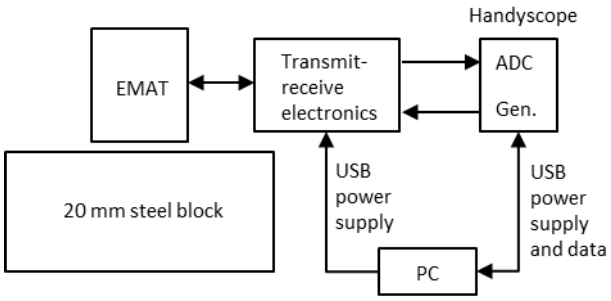

(a)

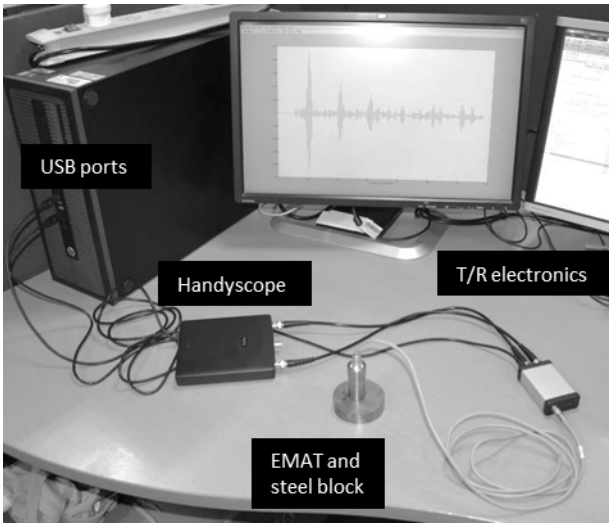

(b)

Fig. 7. Experimental setup using low-power custom-made electronics and sequences with receive intervals to drive a commercial EMAT employing 4.5 Vpp only. (a) Block diagram. (b) Photograph of real setup.

can deliver a maximum of 5 V and 5 W. The electronics consists of a balanced transmitter with a maximum output voltage of 4.5 Vpp and maximum output current of 150 mA, and hence the maximum peak power is less than 0.34 W. The receiver provided a gain of roughly 60 dB and both transmitter and receiver have a bandwidth greater than 5 MHz.

A device (Handyscope-HS5, TiePie, Netherlands) that consists of a signal generator and an analog-to-digital converter (ADC) was employed to drive the custom-made transmitter (driver) and to digitize the output of the custom-made receive amplifier. The Handyscope-HS5 communicates with a PC via the USB port. Both the signal generator and the ADC of the Handyscope-HS5 were sampled at 100 MHz.

In a second setup, the EMAT was connected to the transmit–receive system PowerBox H (Innerspec, USA)—provided by the manufacturer of the EMAT—without changing the EMAT position on the steel block. This setup is not shown for the sake of brevity. The PowerBox H was set to drive the EMAT at 1200 Vpp, which according to the manufacturer can produce a peak power of 8000 W. A 3-cycle pulsed burst at a central frequency of 2.5 MHz was transmitted. The number of averages in the system was set to zero and the repetition rate to 30 bursts/s to avoid any interference from subsequent excitations. The receive amplifier gain was set to 60 dB.

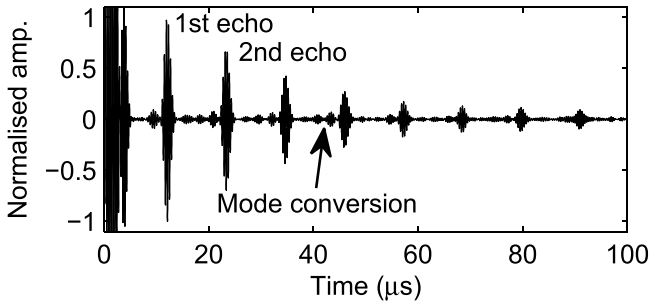

(a) Innerspec system (1200 Vpp).

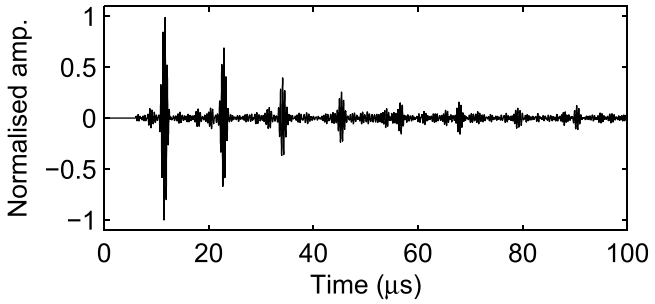

(b) Low-power custom-made system (4.5 Vpp).

Fig. 8. Echoes from 20-mm-thick steel block. (a) Signal from the Innerspec system using 1200-Vpp excitation. (b) Signal from low-power custom-made electronics using a sequence with receive intervals (4.5 Vpp). Signals are normalized to the maximum value of the first echo.

B. Results

The signals obtained using the PowerBox H (Innerspec, USA) were matched filtered with a 3-cycle Hanning window centered at 2.5 MHz to produce a fairer comparison with the cross correlation output of the sequences; the output of the filter is shown in Fig. 8(a). Multiple echoes that correspond to the back and front walls of the steel block can be observed to decay progressively. Smaller echoes produced by mode conversion (from shear to longitudinal waves and vice versa) can also be observed between the main echoes. These mode-converted echoes act as coherent noise, which is dominant over the electrical random noise of the electronics. Therefore, there is not much gain in increasing any further the transmitted power and the length of the sequence or the number of averages in order to increase the SNR, because the coherent noise will increase proportionally.

To drive the custom-made electronics shown in Fig. 7(b), a sequence of length $2^{14} = 16384$ was generated with equal number of receive and transmit intervals randomly distributed, as described in Fig. 3. The sequence burst consisted of a 3-cycle Hanning window centered at 2.5 MHz similarly to the excitation used for the PowerBox H. The length of the sequence intervals was set to six times the burst duration totalling 7.2 μs; this produces a blind zone of roughly 10 mm within a steel specimen when using a shear-wave transducer. This was necessary to permit the energy in the transducer to die out, so that the receive electronics does not saturate. Overall, the total duration of the sequence was 118 ms. The authors argue that a system that processes the data at this rate can be considered quasi-real-time for inspections that use hand-held transducers.

The received signals were zeroed at the transmission intervals to eliminate any noise introduced during this stage and then correlated with the transmitted sequence (see Fig. 3); the results are shown in Fig. 8(b). The first echoes can be clearly identified from the noise threshold. In general, the noise level of Fig. 8(b) appears to be, by visual inspection, just slightly greater than that of Fig. 8(a). This noise could either be noise introduced by the sequence or random electrical noise—the latter mainly due to the receive amplifier. Nonetheless, it is clear that a similar performance can be achieved even with a drastic reduction in the excitation power.

To investigate the performance of the sequence in more detail, an EMAT that produces shear waves linearly polarized [18] was used instead. This EMAT achieves a higher mode purity and a more collimate radiation pattern, so that a thicker sample can be used where the echoes are well separated and mode conversion can be considered negligible. The new specimen is an aluminum block whose dimension is $80 \times 80 \times 150$ mm^3; the transducer was placed in the middle of one of the 80×150 mm^2 faces.

All the parameters remained the same except for the sampling frequency, which was reduced to 20 MHz, so that the acquisition system can handle longer sequences. First, $2^{17} = 131\,072$ signals were averaged; the result is shown in Fig. 9(a), where the inset shows the transmitted burst. The objective was to find a region in the signal where the dominant source of noise corresponds to the receive electronics. Ring down from the coil, noise from the T/R switches and mode conversion can be observed before the first echo, but after the first echo, the noise from the receive electronics dominates. Hence, a good approximation can be obtained by computing the variance of the noise between the first two echoes, as indicated by the horizontal brace.

Fig. 9(b) shows the signals after $N = 2^{14}$ averages and cross correlation with the excitation burst. In this input SNR regime, a signal with the same output SNR can be obtained using a sequence that has a length $L = 2^{16} = 65536$ and intervals six times longer than the transmitted burst, as shown in Fig. 9(c).

The SNR after averaging $N = \{2^{10}, 2^{12}, 2^{14}\}$ signals and convolving the result with the excited burst is shown in Fig. 10 by the circle markers. The SNR produced by sequences of length $L = \{2^{12}, 2^{13}, \ldots, 2^{17}\}$ with intervals six times longer than the transmitted burst is shown by the asterisk markers.

To evaluate (36), so that experimental and theoretical results can be compared, the input SNR, $\mathrm{SNR_{in}}$, was estimated from the SNR of the resulting signal after $N = 2^{14}$ averages by dividing it by the number of averages and the variance of the burst $\sigma_B^2 = 0.26$ and the number of samples of the burst $Q = 25$; this yielded $\mathrm{SNR_{in}} = -19.5$ dB. Also, the variance of the normalized autocorrelation of the burst was $\sigma_{BB}^2 = 0.16$ and the sum of the peak value of the first four echoes normalized to the first one was $\sum_{i=1}^{4} s_i^2 \approx 1.3$. With all this information at hand, the output of (36) is plotted in Fig. 10 for different L values as shown by the continuous line.

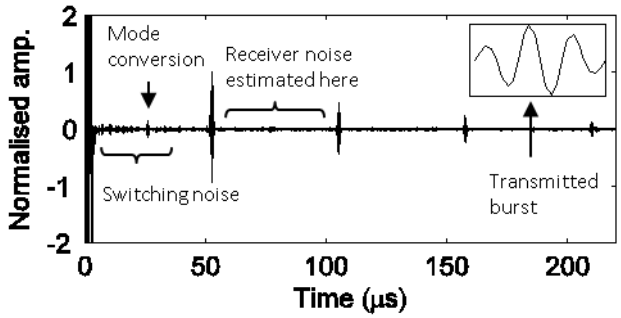

(a) 2^{17} averages.

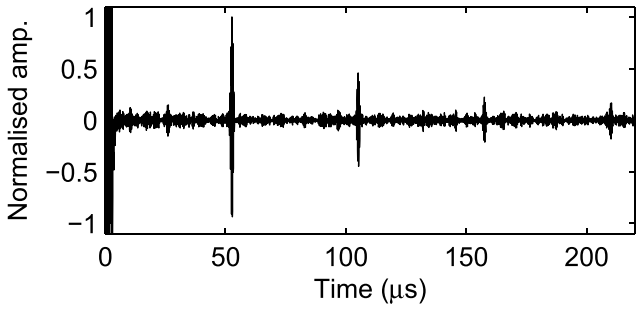

(b) 2^{14} averages.

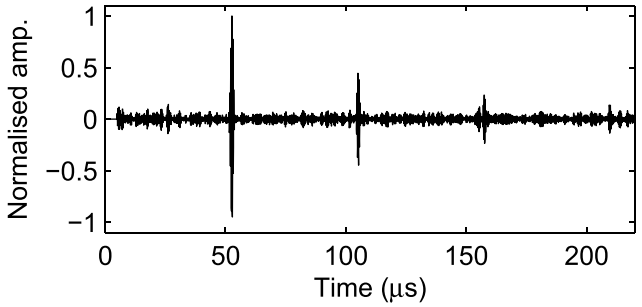

(c) Sequence of length 2^{16}.

Fig. 9. Signals using linearly polarized shear-wave EMAT [18]. (a) 2^{17} averages. Inset: transmitted burst. (b) 2^{14} averages. (c) Sequence of length 2^{16}.

Overall, there is good agreement between the SNRs obtained using averaging, the sequences (with intervals 6 times longer than the burst duration) and (36).

It should be noted that under this low input SNR regime ($\text{SNR}_{\text{in}} = -19.5$ dB), the right-hand term of denominator of (36) is predominant over the left-hand term, and therefore, the noise introduced by the sequence itself is insignificant. Moreover, note that in this case, the increase in the sequence noise due to the multiple reflectors is less than 30%.

C. Discussion of Results

The main conclusion from the experiments is that a significant power reduction in the excitation can be obtained using coded sequences with receive intervals while still being able to obtain a quasi-real-time response. Note that had averaging been used with the custom-made electronics, the wait time between transmissions would have needed to be around 1000 μs and the number of averages needed $2^{12} = 4096$, which corresponds to a total duration of around 4 s (40 times longer than the sequences).

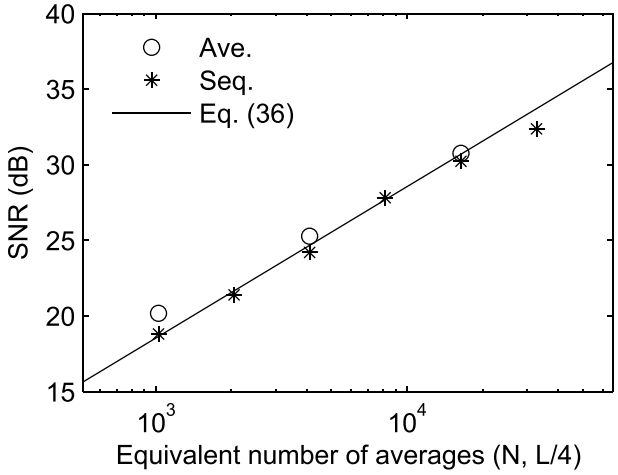

Fig. 10. Experimentally observed SNR versus the number of averages N or equivalent sequence length $L/4$. The input SNR is $\text{SNR}_{\text{in}} = -19.5$ dB.

The power delivered by the PowerBox H was expected to be on the order of 8000 W. A similar signal was obtained by the custom-made electronics driven with the proposed sequences using a mere 0.34 W, which corresponds to a difference of more than 40 dB. The exact power reduction achieved by the custom-made electronics when using the sequences (compared with the PowerBox H) should be interpreted with care because the noise performance of the receive electronics of both systems has a direct impact on the SNR of the received signal; note that the noise performance of the PowerBox H and the custom-made electronics was not compared.

The importance of fast and quiet switching electronics and also of active damping in procuring a short transmission interval should be highlighted. A drawback of the custom-made electronics employed was that the transmission interval was excessively large (six times the duration of the excitation burst). This was necessary to attenuate any remaining energy in the EMAT coil after the excitation and to prevent the receive amplifier from entering into saturation during reception. In this paper, both transmit and receive intervals were set to the same length to simplify the analysis. However, when large transmission intervals are necessary to wait for any ring down or switching noise to die out, it should be considered to only increase the length of those transmit intervals that are followed by a receive interval.

It is also worth mentioning that when the received signals lie close to or below the noise threshold, as in [6], [12]–[16], [18]–[20], and [46], ADCs can be replaced by comparators with negligible (2 dB) loss of information [46], [57]–[59]. This may result in a faster, more compact, and efficient electronics.

VI. Conclusion

Pulse compression has been used for decades to increase the SNR without significantly increasing the overall duration

of the measurement, but current pulse-compression techniques cannot be used in pulse echo when a significant SNR increase is needed and there are close reflectors. This paper presents a solution to that problem, which consists in inserting gaps in a coded sequence where reception can take place.

When the input SNR is low (< 10 dB) or far reflectors are present, the sequences with receive intervals are much faster than averaging or can produce an extra SNR increase for the same overall measurement duration. In general, the sequences can outperform averaging by more than 20 dB in many cases.

We also show that under low input SNR, a simple random codification of the sequence using an equal number of receive and transmit intervals of equal length randomly distributed performs optimally. Moreover, a sequence of any given length can be continuously transmitted without pauses, which increases the refresh rate of the system.

An application of these sequences in industrial ultrasound was presented. It was shown that an EMAT can be driven with 4.5 Vpp obtaining a clear signal in quasi-real-time; commercially available systems require 1200 Vpp for a similar performance.

Future work should be related to the development of fast-switching electronics and the use of the proposed sequences with receive intervals in parallel channels as in medical/industrial ultrasound arrays, where their pseudoorthogonality can be exploited.

ACKNOWLEDGMENT

The authors would like to thank Prof. P. Cawley for the comments on this paper.

REFERENCES

[1] A. S. Mudukutore, V. Chandrasekar, and R. J. Keeler, "Pulse compression for weather radars," *IEEE Trans. Geosci. Remote Sens.*, vol. 36, no. 1, pp. 125–142, Jan. 1998.

[2] M. Parlak, M. Matsuo, and J. F. Buckwalter, "Analog signal processing for pulse compression radar in 90-nm CMOS," *IEEE Trans. Microw. Theory Techn.*, vol. 60, no. 12, pp. 3810–3822, Dec. 2012.

[3] K. Nakahira, T. Kodama, T. Furuhashi, and H. Maeda, "Design of digital polarity correlators in a multiple-user sonar ranging system," *IEEE Trans. Instrum. Meas.*, vol. 54, no. 1, pp. 305–310, Feb. 2005.

[4] Y. T. Tseng, J. J. Ding, and C. S. Liu, "Analysis of attenuation measurements in ocean sediments using normal incidence chirp sonar," *IEEE J. Ocean. Eng.*, vol. 37, no. 3, pp. 533–543, Jul. 2012.

[5] D. Maresca *et al.*, "Intravascular ultrasound chirp imaging," *Appl. Phys. Lett.*, vol. 100, no. 4, p. 043703, 2012.

[6] X. Song, D. Ta, and W. Wang, "A base-sequence-modulated Golay code improves the excitation and measurement of ultrasonic guided waves in long bones," *IEEE Trans. Ultrason., Ferroelect., Freq. Control*, vol. 59, no. 11, pp. 2580–2583, Nov. 2012.

[7] C.-C. Shen and C.-H. Lin, "Chirp-encoded excitation for dual-frequency ultrasound tissue harmonic imaging," *IEEE Trans. Ultrason., Ferroelect., Freq. Control*, vol. 59, no. 11, pp. 2420–2430, Nov. 2012.

[8] C. Yoon, W. Lee, J. H. Chang, T.-K. Song, and Y. Yoo, "An efficient pulse compression method of chirp-coded excitation in medical ultrasound imaging," *IEEE Trans. Ultrason., Ferroelect., Freq. Control*, vol. 60, no. 10, pp. 2225–2229, Oct. 2013.

[9] T. Harrison, A. Sampaleanu, and R. Zemp, "S-sequence spatially-encoded synthetic aperture ultrasound imaging [correspondence]," *IEEE Trans. Ultrason., Ferroelect., Freq. Control*, vol. 61, no. 5, pp. 886–890, May 2014.

[10] S. Mensah, J. Rouyer, A. Ritou, and P. Lasaygues, "Low-contrast lesion detection enhancement using pulse compression technique," *J. Acoust. Soc. Amer.*, vol. 135, no. 4, p. 2156, 2014.

[11] T. Misaridis and J. A. Jensen, "Use of modulated excitation signals in medical ultrasound. Part III: High frame rate imaging," *IEEE Trans. Ultrason., Ferroelect., Freq. Control*, vol. 52, no. 2, pp. 208–219, Feb. 2005.

[12] K. S. Ho, T. H. Gan, D. R. Billson, and D. A. Hutchins, "Application of pulse compression signal processing techniques to electromagnetic acoustic transducers for noncontact thickness measurements and imaging," *Rev. Sci. Instrum.*, vol. 76, no. 5, p. 054902, 2005.

[13] M. P. Mienkina, C.-S. Friedrich, N. C. Gerhardt, W. G. Wilkening, M. R. Hofmann, and G. Schmitz, "Experimental evaluation of photoacoustic coded excitation using unipolar golay codes," *IEEE Trans. Ultrason., Ferroelect., Freq. Control*, vol. 57, no. 7, pp. 1583–1593, Jul. 2010.

[14] T. H. Gan, D. A. Hutchins, D. R. Billson, and D. W. Schindel, "The use of broadband acoustic transducers and pulse-compression techniques for air-coupled ultrasonic imaging," *Ultrasonics*, vol. 39, no. 3, pp. 181–194, 2001.

[15] M. Ricci, L. Senni, and P. Burrascano, "Exploiting pseudorandom sequences to enhance noise immunity for air-coupled ultrasonic nondestructive testing," *IEEE Trans. Instrum. Meas.*, vol. 61, no. 11, pp. 2905–2915, Nov. 2012.

[16] J. E. Michaels, S. J. Lee, A. J. Croxford, and P. D. Wilcox, "Chirp excitation of ultrasonic guided waves," *Ultrasonics*, vol. 53, no. 1, pp. 265–270, 2013.

[17] D. Hutchins, P. Burrascano, L. Davis, S. Laureti, and M. Ricci, "Coded waveforms for optimised air-coupled ultrasonic nondestructive evaluation," *Ultrasonics*, vol. 54, no. 7, pp. 1745–1759, Sep. 2014.

[18] J. Isla and F. Cegla, "Optimization of the bias magnetic field of shear wave EMATs," *IEEE Trans. Ultrason., Ferroelect., Freq. Control*, vol. 63, no. 8, pp. 1148–1160, Aug. 2016, doi: 10.1109/TUFFC.2016.2558467.

[19] B. Yoo, A. S. Purekar, Y. Zhang, and D. J. Pines, "Piezoelectric-paint-based two-dimensional phased sensor arrays for structural health monitoring of thin panels," *Smart Mater. Struct.*, vol. 19, no. 7, p. 075017, 2010.

[20] R. J. Przybyla *et al.*, "In-air rangefinding with an aln piezoelectric micromachined ultrasound transducer," *IEEE Sensors J.*, vol. 11, no. 11, pp. 2690–2697, Nov. 2011.

[21] M. Golay, "Complementary series," *IRE Trans. Inf. Theory*, vol. 7, no. 2, pp. 82–87, Apr. 1961.

[22] C. C. Tseng and C. L. Liu, "Complementary sets of sequences," *IEEE Trans. Inf. Theory*, vol. 18, no. 5, pp. 644–652, Sep. 1972.

[23] R. Sivaswamy, "Multiphase complementary codes," *IEEE Trans. Inf. Theory*, vol. 24, no. 5, pp. 546–552, Sep. 1978.

[24] J. M. Jensen, H. E. Jensen, and T. Hoholdt, "The merit factor of binary sequences related to difference sets," *IEEE Trans. Inf. Theory*, vol. 37, no. 3, pp. 617–626, May 1991.

[25] L. Xu and Q. Liang, "Zero correlation zone sequence pair sets for MIMO radar," *IEEE Trans. Aerosp. Electron. Syst.*, vol. 48, no. 3, pp. 2100–2113, Jul. 2012.

[26] M. Soltanalian and P. Stoica, "Computational design of sequences with good correlation properties," *IEEE Trans. Signal Process.*, vol. 60, no. 5, pp. 2180–2193, May 2012.

[27] Z. Liu, Y. L. Guan, and W. H. Mow, "A tighter correlation lower bound for quasi-complementary sequence sets," *IEEE Trans. Inf. Theory*, vol. 60, no. 1, pp. 388–396, Jan. 2014.

[28] P. Borwein, K. K. S. Choi, and J. Jedwab, "Binary sequences with merit factor greater than 6.34," *IEEE Trans. Inf. Theory*, vol. 50, no. 12, pp. 3234–3249, Dec. 2004.

[29] J. Jedwab, "A survey of the merit factor problem for binary sequences," in *Sequences and Their Applications-SETA*, T. Helleseth, D. Sarwate, H. Y. Song, K. Yang, Eds. Berlin, Germany: Springer, 2005, pp. 30–55.

[30] G. L. Mullen and D. Panario, "What can be used instead of a Barker sequence?" in *Proc. 8th Int. Conf. Finite Fields Appl.*, I. E. Shparlinski Eds, Melbourne, Australia, vol. 461. Jul. 2007. pp. 153–178.

[31] R. H. Barker, *Group Synchronization of Binary Digital Systems in Communication Theory*. New York, NY, USA: Academic, 1953.

[32] K. H. Leung and B. Schmidt, "The field descent method," *Designs, Codes Cryptogr.*, vol. 36, no. 2, pp. 171–188, Aug. 2005.

[33] T. Hoholdt and H. E. Jensen, "Determination of the merit factor of Legendre sequences," *IEEE Trans. Inf. Theory*, vol. 34, no. 1, pp. 161–164, Jan. 1988.

[34] S. W. Golomb and G. Gong, *Signal Design for Good Correlation: For Wireless Communication, Cryptography, Radar*. Cambridge, U.K.: Cambridge Univ. Press, 2005.

[35] H. Torii, M. Nakamura, and N. Suehiro, "A new class of zero-correlation zone sequences," *IEEE Trans. Inf. Theory*, vol. 50, no. 3, pp. 559–565, Mar. 2004.

[36] P. Fan, W. Yuan, and Y. Tu, "Z-complementary binary sequences," *IEEE Signal Process. Lett.*, vol. 14, no. 8, pp. 509–512, Aug. 2007.

[37] M. C. Pérez, J. Ureña, Á. Hernández, A. Jiménez, and C. De Marziani, "Efficient generation and correlation of sequence pairs with three zero-correlation zones," *IEEE Trans. Signal Process.*, vol. 57, no. 9, pp. 3450–3465, Sep. 2009.
[38] J. Song, P. Babu, and D. Palomar, "Sequence design to minimize the weighted integrated and peak sidelobe levels," *IEEE Trans. Signal Process.*, vol. 64, no. 8, pp. 2051–2064, Apr. 15, 2015.
[39] J. Song, P. Babu, and D. P. Palomar, "Optimization methods for designing sequences with low autocorrelation sidelobes," *IEEE Trans. Signal Process.*, vol. 63, no. 15, pp. 3998–4009, Aug. 1, 2015.
[40] P. Stoica, H. He, and J. Li, "New algorithms for designing unimodular sequences with good correlation properties," *IEEE Trans. Signal Process.*, vol. 57, no. 4, pp. 1415–1425, Apr. 2009.
[41] H. He, P. Stoica, and J. Li, "On aperiodic-correlation bounds," *IEEE Signal Process. Lett.*, vol. 17, no. 3, pp. 253–256, Mar. 2010.
[42] W. Nam and S.-H. Kong, "Least-squares-based iterative multipath super-resolution technique," *IEEE Trans. Signal Process.*, vol. 61, no. 3, pp. 519–529, Feb. 1, 2013.
[43] M. Soltanalian, M. M. Naghsh, and P. Stoica, "On meeting the peak correlation bounds," *IEEE Trans. Signal Process.*, vol. 62, no. 5, pp. 1210–1220, Mar. 1, 2014.
[44] C. De Marziani *et al.*, "Modular architecture for efficient generation and correlation of complementary set of sequences," *IEEE Trans. Signal Process.*, vol. 55, no. 5, pp. 2323–2337, May 2007.
[45] E. Garcia, J. Ureña, and J. J. García, "Generation and correlation architectures of multilevel complementary sets of sequences," *IEEE Trans. Signal Process.*, vol. 61, no. 24, pp. 6333–6343, Dec. 15, 2013.
[46] J. Isla and F. Cegla, "The use of binary quantization for the acquisition of low SNR ultrasonic signals: A study of the input dynamic range," *IEEE Trans. Ultrason., Ferroelect., Freq. Control*, vol. 63, no. 9, pp. 1474–1482, Sep. 2012, doi: 10.1109/TUFFC.2016.2571843.
[47] M. Golay, "Sieves for low autocorrelation binary sequences," *IEEE Trans. Inf. Theory*, vol. 23, no. 1, pp. 43–51, Jan. 1977.
[48] T. Hoholdt and J. Justesen, "Ternary sequences with perfect periodic autocorrelation (Corresp.)," *IEEE Trans. Inf. Theory*, vol. IT-29, no. 4, pp. 597–600, Jul. 1983.
[49] A. Gavish and A. Lempel, "On ternary complementary sequences," *IEEE Trans. Inf. Theory*, vol. 40, no. 2, pp. 522–526, Mar. 1994.
[50] R. Craigen and C. Koukouvinos, "A theory of ternary complementary pairs," *J. Combinat. Theory A*, vol. 96, no. 2, pp. 358–375, Nov. 2001.
[51] C. A. Bruce, *Communication Systems: An Introduction to Signals and Noise in Electrical Communication*, 4th ed. Boston, MA, USA: McGraw-Hill, 2002, pp. 388–391.
[52] P. Wilcox, M. Lowe, and P. Cawley, "Omnidirectional guided wave inspection of large metallic plate structures using an EMAT array," *IEEE Trans. Ultrason., Ferroelect., Freq. Control*, vol. 52, no. 4, pp. 653–665, Apr. 2005.
[53] R. Ribichini, F. Cegla, P. B. Nagy, and P. Cawley, "Study and comparison of different EMAT configurations for SH wave inspection," *IEEE Trans. Ultrason., Ferroelect., Freq. Control*, vol. 58, no. 12, pp. 2571–2581, Dec. 2011.
[54] H. Gao, S. Ali, and B. Lopez, "Efficient detection of delamination in multilayered structures using ultrasonic guided wave EMATs," *NDT E Int.*, vol. 43, no. 4, pp. 316–322, Jun. 2010.
[55] F. Li, D. Xiang, Y. Qin, R. B. Pond, Jr., and K. Slusarski, "Measurements of degree of sensitization (DoS) in aluminum alloys using EMAT ultrasound," *Ultrasonics*, vol. 51, no. 5, pp. 561–570, Jul. 2011.
[56] K. Mirkhani *et al.*, "Optimal design of EMAT transmitters," *NDT E Int.*, vol. 37, no. 3, pp. 181–193, Apr. 2004.
[57] A. Derode, A. Tourin, and M. Fink, "Ultrasonic pulse compression with one-bit time reversal through multiple scattering," *J. Appl. Phys.*, vol. 85, no. 9, pp. 6343–6352, 1999.
[58] H. C. Papadopoulos, G. W. Wornell, and A. V. Oppenheim, "Sequential signal encoding from noisy measurements using quantizers with dynamic bias control," *IEEE Trans. Inf. Theory*, vol. 47, no. 3, pp. 978–1002, Mar. 2001.
[59] A. Ribeiro and G. B. Giannakis, "Bandwidth-constrained distributed estimation for wireless sensor networks—Part I: Gaussian case," *IEEE Trans. Signal Process.*, vol. 54, no. 3, pp. 1131–1143, Mar. 2006.

Julio Isla received the engineering degree in telecommunications and electronics (*summa cum laude*) and the M.Sc. degree in radio-electronics from the Instituto Superior Polytechnic José Antonio Echeverría (ISPJAE), Havana, Cuba, in 2009 and 2012, respectively. He is currently pursuing the Ph.D. degree with the Nondestructive Evaluation Group, Imperial College London, London, U.K.

He was with the Bioengineering Department, ISPJAE, from 2009 to 2011, and the Institute of Cybernetics, Mathematics and Physics, Havana, from 2011 to 2013; and with Permasense Ltd., Horsham, U.K., from 2014 to 2016, a company that commercializes the low-power electromagnetic acoustic transducer technology that he developed with colleagues. He has also consulted for other international companies. His current research interests include low-power transduction, arrays, instrumentation, and signal processing.

Frederic Cegla was born in Freiburg im Breisgau, Germany, in 1980. He received the M.Eng. and Ph.D. degrees in mechanical engineering from Imperial College London, London, U.K., in 2002 and 2006, respectively.

He returned to Imperial College London after a short stay as a Post-Doctoral Research Fellow at the University of Queensland, Brisbane, QLD, Australia. In 2008, he joined Imperial College London as Lecturer at the Dynamics section of the Mechanical Engineering Department and in 2014, he was promoted to Senior Lecturer. His current research interests include ultrasonic measurement technology, structural health monitoring, and ultrasonic manipulation of particles and bubbles.

Dr. Cegla was one of the founders of Permasense Ltd., a spin out company that exploits the wall thickness monitoring technology that has been developed by him and his colleagues.